Numerical Analysis of Anode Sheath Structure Shift in an Anode-layer Type Hall Thruster

Shigeru Yokota, Kimiya Komurasaki, and Yoshihiro Arakawa
The University of Tokyo
7-3-1 Hongo, Bunkyo-ku, Tokyo, 113-8656, Japan
yokota@al.t.u-tokyo.ac.jp

Keywords: Hall Thruster, Anode Sheath, PIC-DSMC

Abstract

The anode sheath structure in the hollow anode of an anode-layer type Hall thruster was numerically computed using a fully kinetic 2D3V Particle-in-Cell and Direct Simulation Monte Carlo (PIC-DSMC) code. By treating both ions and electrons as particles, anode surface region, which is electrically non-neutral, was analyzed. In order to analyze in detail, the calculation code was parallelized using Message Passing Interface (MPI). The code successfully simulated the discharge current oscillation. In the low magnetic induction case, ion sheath appears in the anode surface because ionization is enough to maintain the plasma occurs in the anode hollow. As the magnetic induction increases, main ionization region move to outside of the anode. At the same time, anode sheath voltage decreases. In the high magnetic induction case, electron sheath appears on the anode surface periodically because the ionization occurs mainly in the discharge channel.

This anode sheath condition shift can be explained using the simple sheath model.

Introduction

Ionization oscillation in anode layer hall thrusters would be one of the serious problems to be overcome. A hollow anode is commonly used to stabilize the discharge for these thrusters.[1-3] However, the mechanism of discharge stabilization using a hollow anode is still unknown and optimization of anode design has not been done. The goal of our study is to model the sheath structure on the electrode, which has a great effect on the stable discharge of anode layer hall thrusters, and to find out optimum anode design. However, it would be very difficult to measure plasma potential and density inside a hollow anode because plasma density is expected very small and the plasma is electrically non-neutral.

In this study, the structure of electrical sheath inside a hollow anode was numerically simulated using the fully kinetic 2D3V Particle-in-Cell (PIC) and Direct Simulation Monte Carlo (DSMC) methodologies.[4-8] The results are compared with the measurement using a 1-kW class anode layer hall thruster.

Discharge current oscillation

The University of Tokyo anode layer hall thruster has a hollow anode as shown in Fig. 1. It has two guard rings made of stainless steel kept at the cathode potential. The inner and outer diameters of the rings are 48 mm and 62 mm, respectively. Magnetic flux density is variable by changing the current of a solenoid coil set at the center of the thruster.[3,4] Xenon is used as a propellant. A photograph of the hollow anode is shown in Fig. 2. It has an annular hollow anode made of cupper. Z denotes the distance between the channel exit and the anode tip, and D does the width of anode hollow.

Figure 3 shows measured oscillation amplitude Δ of the discharge current and the time-averaged discharge current I_d and B for a certain operation condition. The amplitude was defined as,

$$\Delta = \sqrt{\int_0^\tau \left(I_d - \bar{I}_d\right)^2 dt \Big/ \tau} \qquad (1)$$

The oscillation amplitude was sensitive to the magnetic flux density B and threshold for stable discharge was about 14 mT. Although the oscillation is small at B<14 mT, the thrust efficiency is poor because of large electron backflow current in this range of B. Therefore, the desirable operation condition is limited in a quite narrow range of B**.**

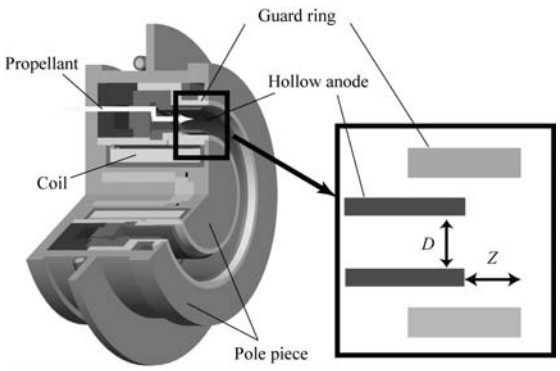

Fig. 1 The University of Tokyo Anode-layer type Hall Thruster.

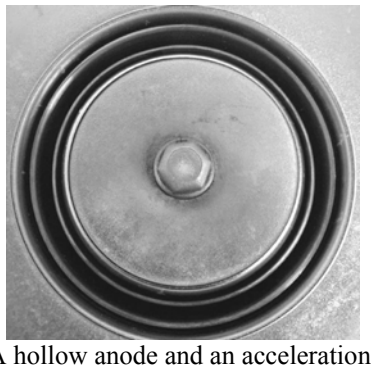

Fig. 2 A hollow anode and an acceleration channel

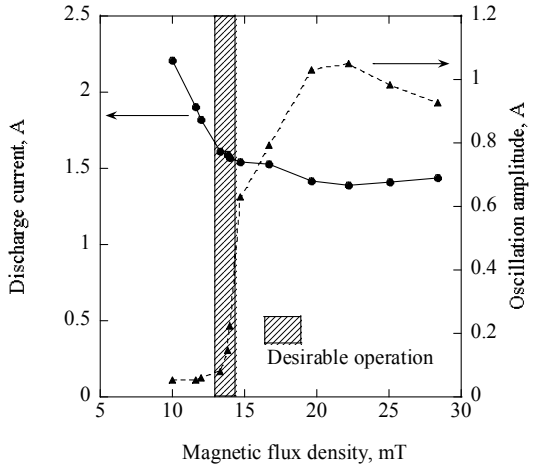

Fig. 3 Oscillation amplitude and average discharge current (V_d=250 V, $e\dot{m}_e/M_e = 1\mathrm{A}_{eq.}$, B_0=20 mT).

Numerical method

Computational model and assumptions

Both electrons and ions are treated as a particle. In the code, 10^6-10^9 of real particles are regarded as one macro-particle and treated kinetically. Only singly charged ionization is considered and mass ratio m_e/m_n is decreased from 4×10^{-6} to 1/100, to speed up the calculation.

Electric and magnetic forces are implemented via the PIC method and collisions are via the DSMC method. The plasma potential φ is calculated using the Poisson's equation as,

$$\frac{\partial^2\phi}{\partial z^2}+\frac{1}{r}\frac{\partial}{\partial r}\left(r\frac{\partial\phi}{\partial r}\right)=-\frac{e}{\varepsilon_0}(n_i-n_e) \qquad (2)$$

Here, r, and z are the cylindrical coordinates and n_i, n_e, e, ε_0 are the ion and electron number density, electronic charge and electric permeability, respectively.

The three highest frequency collisions; Xe – e^- ionization collision, Xe - e^- excitation collision and Xe – e^- elastic scattering are considered. In addition, the Bohm diffusion coefficient is implemented in terms of the virtual collision frequency as

$$\nu_{Bohm}=\frac{1}{16}\frac{eB}{m_e} \qquad (3)$$

Total collision frequency is defined as

$$\nu_{total}=\nu_{ela}+\nu_{ion}+\nu_{exc}+\nu_{Bohm} \qquad (4)$$

The simulation time step is set typically at 1.22×10^{-11} s based on the Larmor frequency that is one order of magnitude larger than the total collision frequency.

Computational grid and boundary conditions

The cylindrical coordinate system (r, z, θ) was used as shown in Fig. 4. Particle's position is expressed in two-dimensional space r and z, while its velocity is expressed in three-dimensional space. That is, particles move in all directions, but the azimuthal coordinate is always discarded.

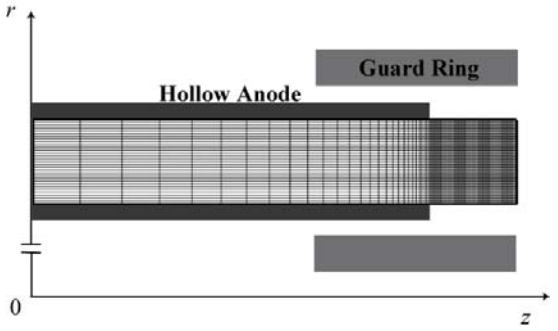

Fig. 4 Computation grid

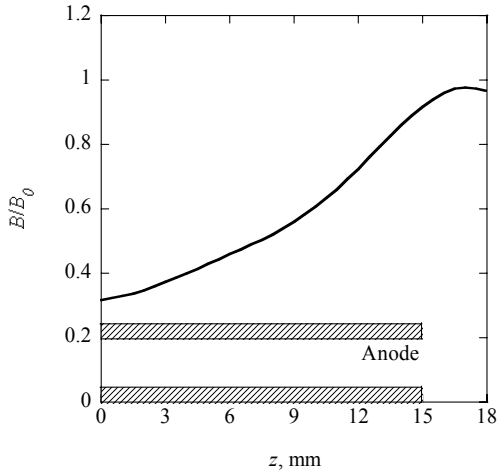

Fig. 5 Radial component of the magnetic flux density distributution.

An orthogonal computational grid is used. In order to observe the sharp density variation in the vicinity of anode exit, the axial cell length is getting smaller toward the anode while the radial cell length is getting smaller toward the anode surface. The minimum cell length is in the order of the Debye length.

Figure 5 shows the magnetic flux density distribution used in the calculation, which is identical to the actual distribution in the thruster. [4] The magnetic flux $2\pi rB(r)$ is constant. B_0 is variable.

Neutral particles are fed from the base of the anode hollow and assumed to be reflected on the anode surface boundary. Electrons are fed from the channel exit boundary with a T_e=10 eV half-Maxwellian velocity distribution. The proper amount of electrons comes into the calculation region automatically by the neutral-electron collision. They reflect on the guard ring boundary, and lost on the anode surface boundary. Ions are produced only by ionization collisions in the computational domain, and lost on every boundary. Ions recombined with electrons on the anode surface return to the channel as neutral particles.

In solving the Poisson's equation, the Dirichlet condition was given on the anode surface and channel exit boundaries and the Neumann condition on the other boundaries.

Result and discussion

Calculation result

Figure 6 shows the ion-production current in the anode hollow and total collision frequency in the anode as a function of *B*. As B increases, ion production current in the anode decreases while the total collision frequency increases. This result deduces main ionization region shifts from the anode hollow to the discharge channel because the electron mobility which depends on the total collision frequency decreases as *B* increases.

Figure 7 shows the potential gap between plasma and anode on the anode tip as a function of *B*. The potential gap decreases with the *B*. In the low *B* case, plasma potential is higher than that of anode because enough ionization occurs in the anode hollow. At the threshold of B, the potential gap vanishes. In the case that *B* is higher than the threshold the plasma potential becomes smaller than the anode potential because electrons should be accelerated to sustain the discharge.

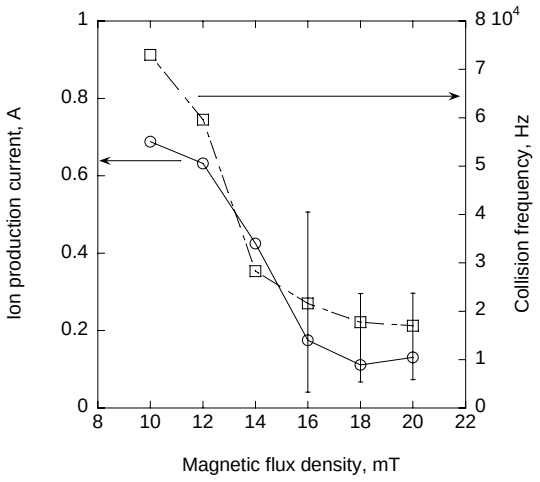

Fig. 6 Ion production current in the anode hollow and total collision frequency as a function of *B*.

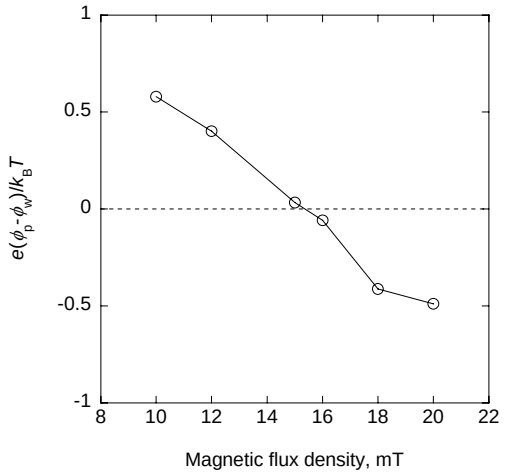

Fig. 7 Potential gap between plasma and anode wall as a function of *B*.

Simple sheath model

Above results can be explained using a simple sheath model. In the sheath region (Fig. 8), Boltzmann relation is assumed

$$v_e = v_{e0} \exp\left[-e\left(\phi_p - \phi_w\right)/k_B T_e\right] , \qquad (5)$$

where,

$$v_{e0} = \sqrt{T_{e0}/2\pi m_e} . \qquad (6)$$

On the other hand, ion velocity is assumed to be the Bohm velocity

$$v_{i0} = \sqrt{T_{e0}/m_i} . \qquad (7)$$

Using the equations (5) - (7) and discharge current (see Fig. 9)

$$I_d = I_e - I_i , \qquad (8)$$

the relation between sheath potential and ion and electron currents

$$\frac{e\left(\phi_p - \phi_w\right)}{k_B T_e} = \ln\left[\sqrt{\frac{m_i}{2\pi m_e}}\frac{I_i}{I_e}\right] \qquad (9)$$

is obtained.

Figure 10 shows the potential gap as a function of I_i/I_e. The calculation result well agrees with this sheath theory.

In the low magnetic induction case, $I_i/I_e > \sqrt{(m_i/2\pi m_e)}$ is satisfied because ion production current in the hollow is enough. Therefore, ion sheath appears ($\phi_p > \phi_w$).

As *B* increases, I_i/I_e decreases with the ionization region shift. At the threshold, $I_i/I_e = \sqrt{(m_i/2\pi m_e)}$.

In the case that *B* is higher than threshold, electron sheath appears because $I_i/I_e < 0\ \sqrt{(m_i/2\pi m_e)}$ is satisfied.

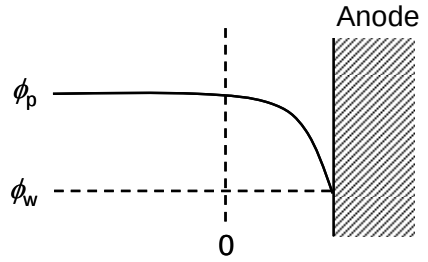

Fig. 8 Schematic of the potential distribution around the anode surface

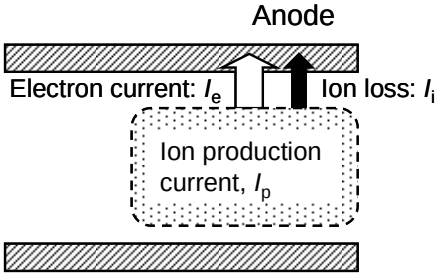

Fig. 9 Schematic of the discharge current

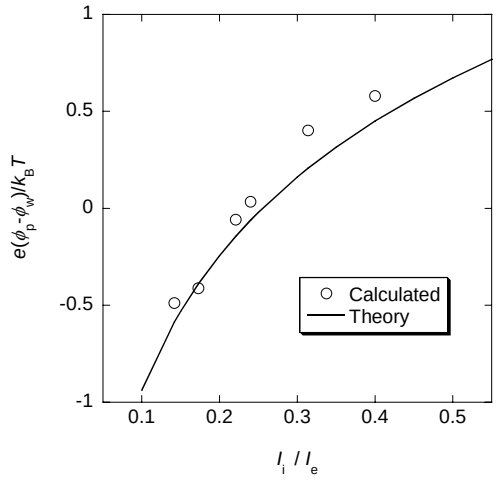

Fig. 10 Potential gap between plasma and anode wall as a function of I_i/I_e.

Nomenclature

B = magnetic flux density
D = anode hollow width
e = electric charge
E = electric field strength
I_d = discharge current
k_B = Boltzmann constant
m = particle mass
n = number density
t = time
T = temperature
v = velocity
V_d = discharge voltage
Z = distance between anode tip and channel exit
ε_0 = free space permeability
ϕ = space potential
ν = collision frequency
r, z, θ = cylindrical coordinate

Suffix

e, i, n = electron, ion, and neutral particle
p = plasma
w = anode wall

Conclusion

A fully kinetic PIC-DSMC code successfully simulated both stable and unstable operation mode of an anode-layer type Hall thruster.

In the low B case (stable mode), ion sheath appeared on the anode surface because ion production current was enough to sustain the discharge.

On the other hand, in the high B case (unstable mode), electron sheath appeared in order to obtain the enough electron current.

The relation between anode sheath shift and ionization region could be explained using a simple one dimensional sheath theory.

References

1) Semenkin A.V., Tverdokhlebov S.O., Garkusha V.I., Kochergin A.V., Chislov G.O., Shumkin B.V., Solodukhin A.V.,Zakharenkov L.E. :Operating Envelopes of Thrusters with Anode Layer, IEPC2001-013, 27th International Electric Propulsion Conference, Pasadena, USA, October 2001.
2) Semenkin, A., Kochergin, A., Garkusha, V., Chislov, G., Rusakov, A. :RHETT/EPDM Flight Anode Layer Thruster Development, IEPC-97-106, 25th International Electric Propulsion Conference, Cleveland, USA, August 1997.
3) Yamamoto, N., Nakagawa, T., Komurasaki, K., Arakawa, Y. :Effect of Discharge Oscillations on Hall Thruster Performance, ISTS 2002-b-17, 23rd the International Symposium on Space Technology and Science, Shimane, Japan, May 2002.
4) Yasui, S., Yamamoto, N., Komurasaki, K., Arakawa, Y. :Effect of Sheath Structure on Operating Stability in an Anode Layer Thruster," Proceedings of Asian Joint Conferences in Propulsion and Power 2004, pp.382-387, Seoul, Korea, March 2004.
5) Hirakawa, M., Aralawa, Y. :Particle Simulation of Plasma Phenomena in Hall Thrusters, IEPC-95-164, 24th International Electric Propulsion Conference, Moscow, Russia, September 1995
6) Szabo, J. J. :Fully Kinetic Hall Thruster Modeling of a Plasma Thruster, PhD Thesis, Massachusetts Institute of Technology, 2001
7) Szabo, J., Rostler, P. :One and Two Dimensional Modeling of the BHT-1000", IEPC-02-231, 28th International Electric Propulsion Conference, Toulouse, France, March 2003.
8) Kumakura, K., Yasui, S., Komurasaki K., Arakawa, Y. :Plasma Modeling of a Hollow Anode for an Anode Layer Type Hall Thruster" IEPC-02-086, 28th International Electric Propulsion Conference, Toulouse, France, March 2003.